IEEE Photonics Journal
An IEEE Photonics Society Publication

Silicon Add-Drop Filter Based on Multimode Grating Assisted Couplers

Volume 8, Number 6, December 2016

Huiye Qiu
Yuxia Su
Fuzhong Lin
Jianfei Jiang
Ping Yu
Hui Yu
Jianyi Yang
Xiaoqing Jiang

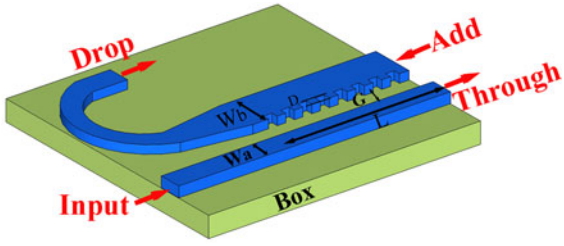

DOI: 10.1109/JPHOT.2016.2625268
1943-0655 © 2016 IEEE

Silicon Add-Drop Filter Based on Multimode Grating Assisted Couplers

Huiye Qiu,[1] Yuxia Su,[1] Fuzhong Lin,[1] Jianfei Jiang,[3] Ping Yu,[2] Hui Yu,[3] Jianyi Yang,[3] and Xiaoqing Jiang[3]

[1]Department of Mechanical and Electrical Engineering, Longyan University, Longyan 364012, China
[2]Ningbo Institute of Technology, Zhejiang University, Ningbo 315100, China
[3]Department of Information Science and Electronics Engineering, Zhejiang University, Hangzhou 310027, China

DOI:10.1109/JPHOT.2016.2625268

Manuscript received October 3, 2016; revised October 27, 2016; accepted November 1, 2016. Date of publication November 4, 2016; date of current version November 17, 2016. This work was supported in part by the Fund of the Nature Basic Research Program of China under Grant 2013CB632105, in part by the National Natural Science Foundation of China under Grant 61307074 and Grant 61405177, in part by the Fujian Province Science Foundation of China under Grant 2015J01658, in part by the Ningbo Natural Science Foundation under Grant 2014A610150, in part by Natural Science Foundation of Zhejiang Province under Grant LY17F050008, and in part by Longyan University Science Foundation under Grant 2014019. Corresponding author: H. Qiu (e-mail: qiuhuiye@lyun.edu.cn).

Abstract: We demonstrate the design, fabrication, and characterization of a two-mode silicon add-drop filter, which is based on multimode grating-assisted contra-directional couplers. The mode conversions between two asymmetry strip waveguides are realized by using spatially periodic corrugations in one side wall of a multimode waveguide at the phase-match condition. Experimental results show that the fundamental mode of a single-mode waveguide is successfully coupled to the first two modes of the multimode waveguide in the opposite direction. The corresponding mode conversion bandwidths and extinction ratios are also measured. The demonstrated add-drop filter may find their applications in a hybrid multiplexing system by combing wavelength-division multiplexing technology and mode-division multiplexing technology for on-chip optical interconnect.

Index Terms: Integrated optics device, gratings, wavelength filtering devices, Bragg reflectors, waveguides.

1. Introduction

Silicon photonics devices are desirable for the realization of on-chip optical interconnections with high capacity for their compatibility with a standard complementary metal-oxide-semiconductor (CMOS) technology [1]. As an important component of wavelength division multiplexing (WDM) systems, various add-drop filters have been developed for silicon-on-insulator (SOI) platform, such as Bragg gratings, ring-resonators and contra-directional couplers (contra-DCs). Bragg gratings have perfect spectral characteristics for (de)multiplexing in a WDM system [2]–[5]. However, they are two-port devices and require a circulator in the system. Ring-resonator add-drop filters have received much attention for their compact size and various applications [6], [7], but they are limited by relatively small free spectral ranges (FSR). Contra-DCs are grating assisted add-drop filters and have shown their good properties as an add-drop filter in a WDM system [8]–[12]. However, conventional Contra-DCs usually consist of two asymmetry single-mode waveguides, which support only two fundamental compound modes and thus one mode channel.

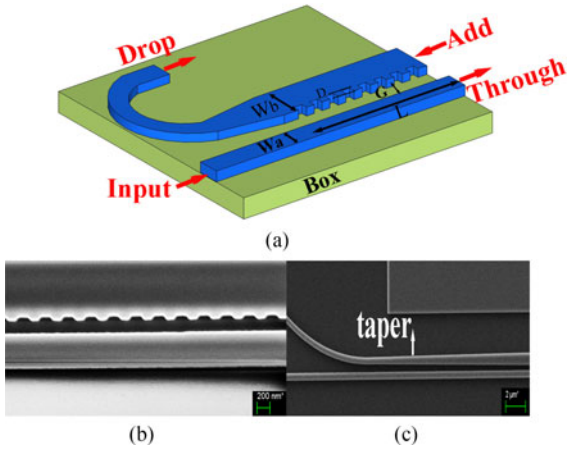

Fig. 1. (a) Three-dimensional view of the proposed MGACCs. The SEM image of the (b) coupling part (c) tapered waveguide.

Mode-division multiplexing (MDM) technology is a good way to expand the capacity of a single photonics link without increasing too much footprint and complexity of the system [13], [14]. Recently, Bragg gratings based on multimode silicon waveguides have attracted a lot of interests due to their unique features [15]–[17]. The fundamental mode of a single mode waveguide is coupled into an adjacent multi-mode waveguide grating at the wavelength of interest by using Contra-DCs [16]. An integrated space-division multiplexing (SDM) is proposed on a chip with small device footprint and high packing density by cascading multiple contra-DCs [17]. In this paper, we design and fabricate a two-mode silicon add-drop filter based on multimode grating-assisted contra-directional couplers (MGACCs) on the SOI platform. In our device, the fundamental mode of a single-mode strip waveguide is coupled to the TE_0 and TE_1 modes of a multimode strip waveguide with different designed Bragg grating periods, respectively. A tapered waveguide is designed to distinguish and convert the TE_0 and TE_1 modes. In order to drop the TE_1 mode in the multimode waveguide, another MGACCs is cascaded. The experimental results show that the modes conversions between the two waveguides are realized successfully. The proposed device can combine its WDM functionalities with MDM capabilities to further augment the multiplexing capacity of the device.

2. Device Design and Analysis

The proposed MGACCs is schematically illustrated in Fig. 1(a). The device consists of two asymmetry parallel strip waveguides on the top of SiO_2 box layer. The cladding layer is air. Waveguide *a* supports only TE_0 mode, while waveguide *b* supports two TE modes. The corrugations in waveguide *b* are placed in one sidewall, which faces the straight waveguide *a*. The corrugated waveguide *b* is used as the add-drop port, and the straight waveguide *a* is used as the input-through port. The widths of the two strip waveguides, which are separated by a gap with a width of *G,* are *Wa* and *Wb*, respectively. An adiabatic taper connects the MGACCs with a single-mode waveguide at the drop-port.

When light is input from the straight waveguide *a* (see Fig. 1), the forward cross-coupling between the two waveguides is negligible due to the phase mismatch caused by the width difference. Meanwhile, the contra-directional coupling can be realized by the spatially periodic corrugation at the phase-match condition [15]

$$\lambda/\Lambda = (n_a + n_{bi}) \quad (i = 0, 1) \tag{1}$$

where n_a and n_b represent the TE mode effective indices of waveguides *a* and *b*, respectively, *i* is the mode order, Λ is the grating period, and λ is the Bragg wavelength.

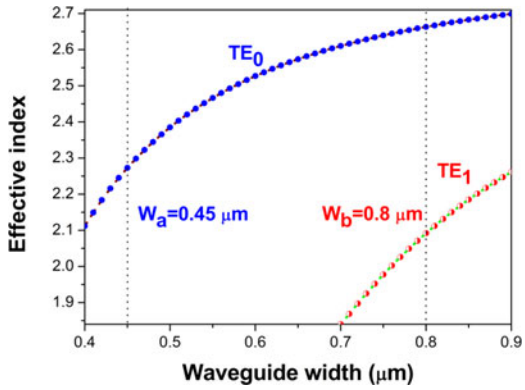

Fig. 2. Relationships between effective index and waveguide width.

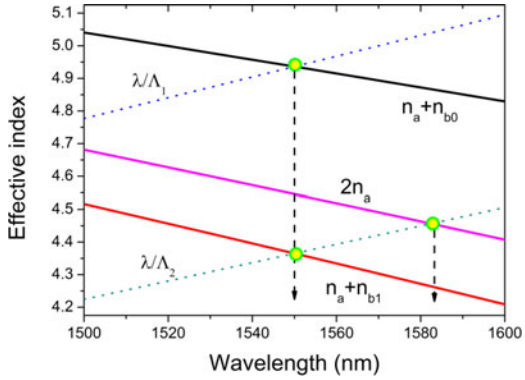

Fig. 3. Calculated effective indices of the modes with the phase-match condition. (n_a, n_{b0}, and n_{b1} are the effective indices of the fundamental mode of the input waveguide and the first two modes of the multimode waveguide.)

By designing the grating period, one can couple the TE_0 mode of the input waveguide to the TE_0 and TE_1 modes of the multimode waveguide, respectively. When the dropped TE_0 mode in the multimode waveguide propagates through the tapered waveguide, it will then be adiabatically transited into a forward propagating fundamental mode of the drop waveguide. On the contrary, the dropped TE_1 mode will be radiated once it enters into the drop waveguide, as the drop waveguide supports only the fundamental mode. Thus we can ensure that only the TE_0 mode could be output at the drop-port. To drop the TE_1 mode, we could cascade another MGACCs before the taper.

In our device, the thickness of the silicon strip waveguides is chosen to be 220 nm. Fig. 2 shows the effective index as a function of waveguide width for the first two mode orders at the wavelength of 1550 nm. The straight waveguide has a width of 0.45 μm, while the width of the multimode waveguide is chosen to be 0.8 μm to support two TE modes. The coupling gap *G* is set to be 200 nm, the corrugation width D is 50 nm, the duty cycle of the Bragg gratings is 50%, and the coupling length *L* is 500 μm.

The solid and dotted lines in Fig. 3 are the plots of the right-hand side and left-hand side of the (1), as a function of the wavelength, respectively. Therefore, the cross points of the solid and dotted lines represent the phase-match condition. We choose the values of Λ for effective contra-directional coupling at the wavelength of 1550 nm. It is observed that in the device, a larger value of Λ is needed for higher order mode as the sum of n_a and n_b decreases. The calculation results show that the grating periods for coupling from the fundamental mode of the input waveguide to the TE_0 and TE_1 modes of the multimode waveguide are $\Lambda_1 = 314$ nm and $\Lambda_2 = 356$ nm, respectively. The phase-match condition for the inter-coupling in the input waveguide, i.e., $\lambda/\Lambda = 2n_a$, is also plotted

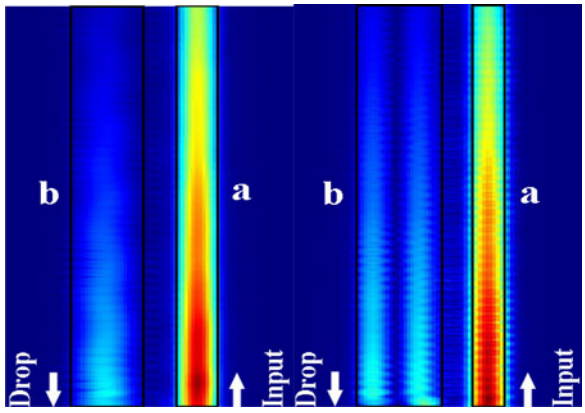

Fig. 4. Three-dimensional FDTD simulations of the MGACCs for light coupling from the straight input waveguide *a* at the wavelength of 1550 nm to (a) the TE0 mode and (b) the TE1 mode in the multimode waveguide *b*.

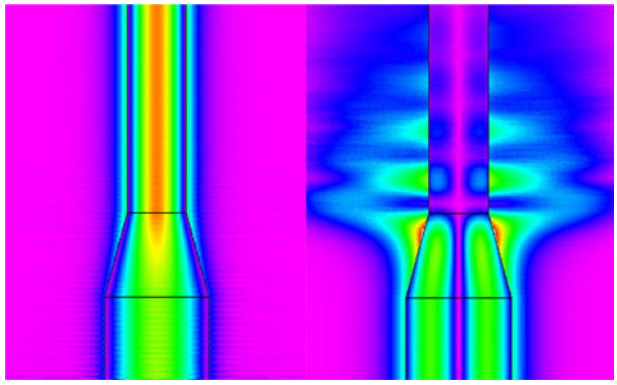

Fig. 5. Light propagation along the designed taper for (a) the TE_0 mode and (b) the TE_1 mode in the multimode waveguide.

in Fig. 3. It can be observed that the Bragg wavelength is far beyond 1550 nm, when we select the grating periods of 314 nm and 356 nm, respectively. Therefore, we can design two grating couplers to couple the fundamental modes of two input waveguides to the TE_0 and TE_1 modes of the bus multimode waveguide at the same wavelength, respectively. In our work, we fabricated two devices for the two modes conversions, respectively. It is worth pointing out that the inter-coupling in the input waveguide is greatly suppressed, as the corrugations are designed far away from the input waveguide [8].

In order to better understand this concept, we perform 3-D finite-difference time-domain (FDTD) simulations. In view of the computation time and memory, we set a short coupling length of only 10 μm. The mode conversions between the input waveguide and the multimode waveguide are calculated by a 3-D-FDTD simulation tool, as presented in Fig. 4. Fig. 4(a) and 4(b) show that the fundamental mode of the input waveguide is contra-directionally coupled to the TE_0 and TE_1 mode in the multimode waveguide at the wavelength of 1550 nm, respectively.

A 20-μm–length tapered waveguide with the core width varying from 0.8 μm to 0.45 μm is designed to modify the mode size at the multimode waveguide. The simulation of the light propagating from the multimode waveguide to a single-mode drop waveguide via the taper is illustrated in Fig. 5 by using beam propagation method (BPM). As seen from Fig. 5(a), when the TE_0 mode passes through the tapered waveguide, it adiabatically transits into the fundamental mode of the drop waveguide. On the other hand, when the TE_1 mode light reaches the tapered waveguide, it totally transits into the radiation mode and dissipates, as shown in Fig. 5(b). It is due to that the TE_1 mode

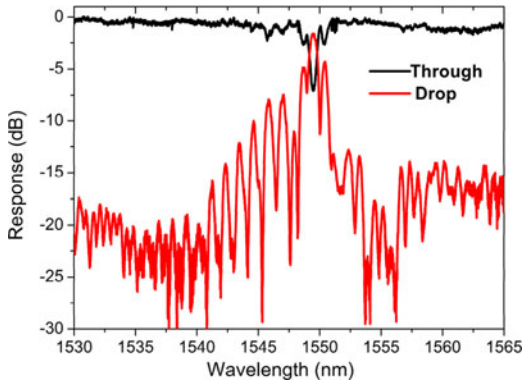

Fig. 6. Normalized through-port and drop-port spectra for contra-directional coupling from the fundamental of the input waveguide to the TE_0 mode of the multimode waveguide.

and the fundamental mode of the drop waveguide are mismatched. Therefore, we can determine the order of the dropped mode in the multimode waveguide by measuring the power at the through port and drop port.

3. Experimental Results and Discussion

The proposed GMACCs are fabricated on an SOI wafer with a 220-nm-thick top silicon layer and a 3-μm-thick buried oxide layer. In the experiment, E-beam lithography (Vistec EBPG 5200) was used to define the structures on the ZEP520A resist. Then the patterns were transferred to the top silicon layer by inductively coupled plasma (ICP) dry etching using SF6 and C4F8 gases. To share the same etching depth as the strip waveguide, we employ photonics crystal based grating couplers. The scanning electron microscopy (SEM) image of the fabricated GMACCs and tapered waveguide are shown in Fig. 1(b) and (c). In the measurements, the TE-polarized lights from a tunable laser (SANTEC, TSL-510) were coupled into/out of the chip by grating couplers. The output spectra were measured by an optical power detector and power meter (HP, 8153a).

To verify the operation principle, we at first characterize the mode conversion between the fundamental mode of the input waveguide and the TE_0 mode of the multimode waveguide. Fig. 6 shows the measured normalized through port and drop port spectra with the designed grating period $\Lambda = 314$ nm. The coupling loss of the two grating couplers has been normalized. As seen from Fig. 6, when light is launched at the input port, the contra-directional coupling occurs at the central wavelength of 1550 nm. As the device has a slight corrugation depth of 50 nm and large coupling gap of 200 nm, the coupling strength is weakened. Therefore, the add drop filter shows good wavelength selectivity with a measured bandwidth of $\sim$0.8 nm. One could obtain a broad bandwidth by enhancing the coupling coefficient, such as larger corrugation depth or narrower coupling gap [11]. The extinction ratio is -7.2 dB at the resonant wavelength, which can be increased by extending the coupling length since the extinction ratio is a function of both the coupling coefficient and the coupling length [18]. The insertion loss of -1.2 dB at the central wavelength for the drop port spectrum is also measured. Owing to the uniform corrugations, the device has undesirable sideband lobes in the spectra, which can be compressed in future by apodization [19]. There is no other notch in the spectrum throughout the scanned wavelength range, which implies no inter-coupling in the input waveguide occurs.

Then, the mode coupling between the fundamental mode of the input waveguide and the TE_1 mode of the multimode waveguide is demonstrated with the designed grating period of 356 nm. As shown in Fig. 7, in the through-port spectrum, there is a resonant notch with a bandwidth of $\sim$2.3 nm and an extinction ratio of -18 dB at the central wavelength of 1560 nm. However, the relevant peak is not measured at the drop port spectrum. In order to investigate the coupling mode at the resonant wavelength, an optical fiber circulator is used to measure the reflection power at

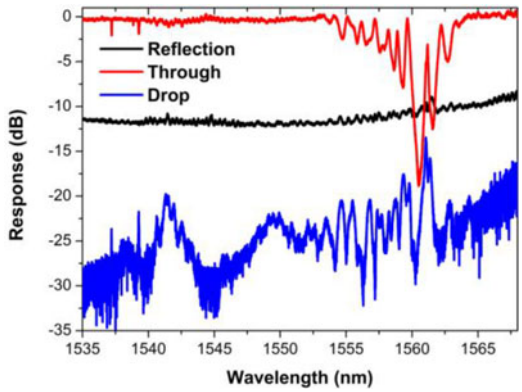

Fig. 7. Normalazed through port and drop port spectra for contra-directional coupling from the fundamental mode of the input waveguide to the TE_1 mode of the multimode waveguide.

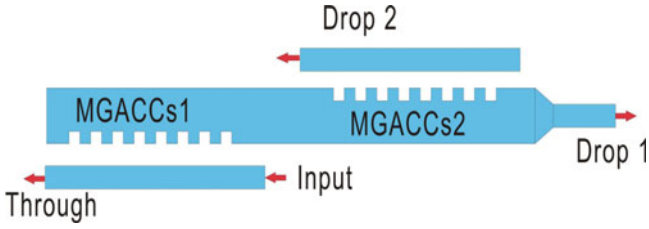

Fig. 8. Pair of GMACCs for the TE_1 mode coupling in the multimode waveguide.

the input port. It can be seen that there is no resonance in the reflection spectrum (see the black line in Fig. 7). Therefore, we believe that the resonance in the through-port spectrum is not caused by the intra-waveguide Bragg reflection. From the drop port spectrum, one can see the power around the resonant wavelength is lower than -20 dB. According to the analysis, we confirm that the fundamental mode of the input waveguide is coupled to the TE_1 mode of the multimode waveguide and the TE_1 mode power finally dissipates when passing through the taper. In addition, one can see that the bandwidth and extinction ratio of the TE_1 mode coupling in the through port spectrum are larger than those in Fig. 6, which means the coupling coefficient between the fundamental mode and the TE_1 mode of the multimode waveguide is larger. The results agree well with our conclusions in [15].

Higher order modes of multimode waveguides are usually converted to the fundamental mode of a single-mode waveguide before they are measured. There are a lot of ways to achieve this conversion, such as directional couplers (DCs) [20], [21]. Contra-DCs [15], asymmetric Y-junctions [22]–[24], or adiabatic couplers [25]. In our device, a pair of MGACCs is design to couple the fundamental mode of the input waveguide to the TE_1 mode of the multimode waveguide, and then the TE_1 mode is converted to the fundamental mode of a single-mode drop waveguide, as shown in Fig. 8. Both of the two MGACCs have the same parameters. In order to enhance the coupling strength, the MGACCs have a large corrugation depth of 100 nm and a narrow coupling gap of 150 nm, respectively.

Fig. 9 illustrates the measured transmission spectra at the through and drop ports after normalizing the insertion loss of the grating coupler. From the spectrum of the through port (black line in Fig. 9), one can see that the mode coupling between the fundamental mode of the input waveguide and the TE_1 mode of the multimode by MGACCs1, is greatly strengthened, as a broad bandwidth of about 13 nm and an high extinction ratio of over -21 dB are measured. The spectrum at the second drop port demonstrates that the TE_1 mode in the multimode waveguide is coupled to the fundamental mode in the second drop waveguide. The spectrum does not match well with that at the

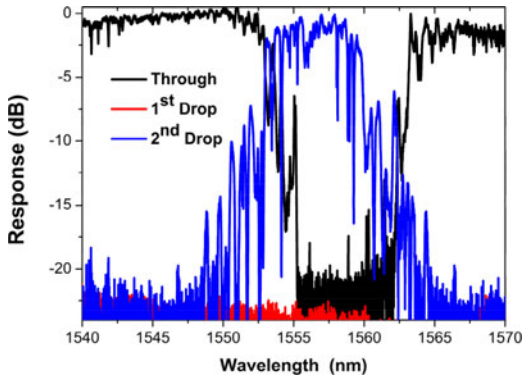

Fig. 9. Normalized through port and drop port spectra for the mode conversions from the fundamental mode of the input waveguide to the TE_1 mode of the multimode waveguide and finally to second drop waveguide.

through-port with a ~3 nm blue shift. Therefore, the bandwidth of the spectrum decreases to about 10 nm. We attribute this to that the resonant Bragg wavelength of MGACCs2 shifts to the blue wavelength. The difference of the Bragg wavelengths is because that the two fabricated MGACCs are not totally same. There are some undesired abnormal oscillations in the spectrum, which is due to the phase noise caused by the fabrication errors and waveguide sidewall roughness. We could improve our device by more careful fabrication. The spectrum at the first drop-port is also measured, and the result shows that the crosstalk between the two drop ports is larger than 22 dB at the wavelength of 1559 nm. It is worth to point out that more mode channels can be achieved by cascading more pairs of GMACCs.

4. Conclusion

In summary, we have proposed a two-mode add-drop filter based on GMACCs. The design, analysis and fabrication of the device are demonstrated. By using the GMACCs, the fundamental mode of the input waveguide could be coupled to the TE_0 and TE_1 modes of the multimode waveguide, respectively. The TE_1 mode conversion is observed to have a stronger coupling coefficient with larger bandwidths and higher extinction ratios than that of TE_0 mode. The measured results show that the designed filter have the potentiality to be used in WDM and MDM systems for on-chip optical interconnect.

Reference

[1] A. Shacham, K. Bergman, and L. P. Carloni, "Photonic networks-on -chip for future generations of chip multiprocessors," *IEEE Trans. Comput.*, vol. 57, no. 9, pp. 1246–1260, Sep. 2008.
[2] D. T. H. Tan, K. Ikeda, and Y. Fainman, "Cladding-modulated Bragg gratings in silicon waveguides," *Opt. Lett.*, vol. 34, no. 9, pp. 1357–1359, May 2009.
[3] X. Wang, W. Shi, H. Yun, S. Grist, N. A. F. Jaeger, and L. Chrostowski, "Narrow-band waveguide Bragg gratings on SOI wafers with CMOS-compatible fabrication process," *Opt. Exp.*, vol. 20, no. 14, pp. 15547–15558, Jun. 2012.
[4] D. T. H. Tan, K. Ikeda, R. E. Saperstein, B. Slutsky, and Y. Fainman, "Chip-scale dispersion engineering using chirped vertical gratings," *Opt. Lett.*, vol. 33, no. 24, pp. 3013–3015, Dec. 2008.
[5] G. Jiang, R. Chen, Q. Zhou, J. Yang, M. Wang, and X. Jiang, "Slab-modulated sidewall Bragg gratings," *IEEE Photon. Technol. Lett.*, vol. 23, no. 1, pp. 6–8, Jan. 2011.
[6] V. R. Almeida, C. A. Barrios, R. R. Panepucci, and M. Lipson, "All-optical control of light on a silicon chip," *Nature*, vol. 431, no. 28, pp. 1081–1084, Oct. 2004.
[7] T. Hu *et al.*, "Wavelength-selective 4×4 nonblocking silicon optical router for networks-on-chip," *Opt. Lett.*, vol. 36, no. 23, pp. 4710–4712, Dec. 2011.
[8] H. Qiu *et al.*, "FSR-free add-drop filter based on silicon grating-assisted contradirectional couplers," *Opt. Lett.*, vol. 38, no. 1, pp. 1–3, Jan. 2013.

[9] W. Shi, X. Wang, W. Zhang, L. Chrostowski, and N. A. F. Jaeger, "Contradirectional couplers in silicon-on-insulator rib waveguides," *Opt. Lett.*, vol. 36, no. 20, pp. 3999–4001, Oct. 2011.
[10] W. Shi *et al.*, "Ultra-compact, flat-top demultiplexer using anti-reflection contra-directional couplers for CWDM networks on silicon," *Opt. Exp.*, vol. 21, no. 6, pp. 6733–6738, Mar. 2013.
[11] Y. Zhang *et al.*, "High-extinction-ratio silicon polarization beam splitter with tolerance to waveguide width and coupling length variations," *Opt. Exp.*, vol. 24, no. 6, pp. 6586–6593, Mar. 2016.
[12] L. Chrostowski and M. Hochberg, *Silicon Photonics Design*. Cambridge, U.K.: Cambridge Univ. Press, 2014.
[13] D. Dai, J. Wang, and Y. Shi, "Silicon mode (de)multiplexer enabling high capacity photonic networks-on-chip with a single-wavelength-carrier light," *Opt. Lett.*, vol. 38, no. 9, pp. 1422–1424, May 2013.
[14] D. Dai, J. Wang, S. Chen, S. Wang, and S. He, "Monolithically integrated 64-channel silicon hybrid demultiplexer enabling simultaneous wavelength- and mode-division-multiplexing," *Laser Photon. Rev.*, vol. 9, no. 3, pp. 339–344, May 2015.
[15] H. Qiu *et al.*, "Silicon mode multi/demultiplexer based on multimode grating-assisted couplers," *Opt. Exp.*, vol. 21, no. 15, pp. 17904–17911, Jul. 2013.
[16] G. F. R Chen, T. Wang, K. J. A. Ooi, A. K. L. Chee, L. K. Ang, and D. T. H. Tan, "Wavelength selective mode division multiplexing on a silicon chip," *Opt. Exp.*, vol. 23, no. 6, pp. 8095–8103, Mar. 2015.
[17] A. Grieco, G. Porter, and Y. Fainman, "Integrated space-division multiplexer for application to data center networks," *IEEE J. Sel. Topics Quantum Electron.*, vol. 22, no. 6, Nov. 2016, Art. no. 8200106.
[18] P. Yeh and H. F. Taylor, "Contradirectional frequency-selective couplers for guided-wave optics," *Appl. Opt.*, vol. 19, no. 16, pp. 2848–2855, Aug. 1980.
[19] J. St-Yves, H. Bahrami, P. Jean, S. LaRochelle, and W. Shi, "Widely bandwidth-tunable silicon filter with an unlimited free-spectral range," *Opt. Lett.*, vol. 40, no. 23, pp. 5471–5474, Dec. 2015.
[20] L. W. Luo *et al.*, "WDM-compatible mode-division multiplexing on a silicon chip," *Nat. Commun.*, vol. 5, Jan. 2014, Art. no. 3069.
[21] D. Dai, "Silicon mode-(de)multiplexer for a hybrid multiplexing system to achieve ultrahigh capacity photonic networks-on-chip with a single-wavelength-carrier light," in *Proc. Asia Commun. Photon. Conf.*, 2012, paper ATh3B.3.
[22] W. Chen, P. Wang, and J. Yang, "Mode multi/demultiplexer based on cascaded asymmetric Y-junctions," *Opt. Exp.*, vol. 21, no. 21, pp. 25113–25119, Oct. 2013.
[23] J. D. Love and N. Riesen, "Single-, few-, and multimode Y-junctions," *J. Lightw. Technol.*, vol. 30, no. 3, pp. 304–309, Feb. 2012.
[24] H. Qiu *et al.*, "Silicon band-rejection and band-pass filter based on asymmetric Bragg sidewall gratings in a multimode waveguide," *Opt. Lett.*, vol. 41, no. 11, pp. 2450–2453, 2016.
[25] Y. Ding, J. Xu, F. Da Ros, B. Huang, H. Ou, and C. Peucheret, "On-chip two-mode division multiplexing using tapered directional coupler-based mode multiplexer and demultiplexer," *Opt. Exp.*, vol. 21, no. 8, pp. 10376–10382, Apr. 2013.